Virus Research 270 (2019) 197642

Contents lists available at ScienceDirect

Virus Research

journal homepage: www.elsevier.com/locate/virusres

Molecular characterization of a novel reassortment *Mammalian orthoreovirus* type 2 isolated from a Florida white-tailed deer fawn

Mohammad Shamim Ahasan[a,b,c], Kuttichantran Subramaniam[a,b], Katherine A. Sayler[d], Julia C. Loeb[b,e], Vsevolod L. Popov[f], John A. Lednicky[b,e], Samantha M. Wisely[d], Juan M. Campos Krauer[d,g], Thomas B. Waltzek[a,b,*]

[a] Department of Infectious Diseases and Immunology, College of Veterinary Medicine, University of Florida, Gainesville, FL, USA
[b] Emerging Pathogens Institute, University of Florida, Gainesville, FL, USA
[c] Faculty of Veterinary and Animal Sciences, Hajee Mohammad Danesh Science and Technology University, Dinajpur, RG, Bangladesh
[d] Department of Wildlife Ecology and Conservation, University of Florida, Gainesville, FL, USA
[e] Department of Environmental and Global Health, College of Public Health and Health Professions, University of Florida, Gainesville, FL, USA
[f] Department of Pathology, University of Texas Medical Branch, Galveston, TX, 77555, USA
[g] Department of Large Animal Clinical Sciences, College of Veterinary Medicine, University of Florida, Gainesville, FL, USA

ARTICLE INFO

Keywords:
Mammalian orthoreovirus
Reoviridae
Deer farming
White-tailed deer
Odocoileus virginianus

ABSTRACT

Mammalian orthoreovirus (MRV) is the type species of the genus *Orthoreovirus* and causes a range of significant respiratory, nervous or enteric diseases in humans and animals. In 2016 a farmed white-tailed deer (*Odocoileus virginianus*) fawn became ill, displaying clinical signs of lethargy, dehydration, and profuse foul-smelling diarrhea. A necropsy was performed after the three-week-old fawn died and various tissue samples were submitted to the University of Florida's Cervidae Health Research Initiative for diagnostic evaluation. Aliquots of homogenized heart, liver, and spleen tissues were inoculated onto Vero E6 cells. After virus-specific cytopathic effects (CPE) were detected in Vero cells inoculated with spleen homogenate, infected cells were fixed in glutaraldehyde and analyzed by transmission electron microscopy (TEM), which revealed icosahedral virus particles approximately 75 nm in diameter with morphologies consistent with those of reoviruses within the cytoplasm of the infected cells. RNA extracted from virions in the spent media of infected cells with advanced CPE was used to prepare a cDNA library, which was sequenced using an Illumina MiSeq sequencer. Complete coding sequences for ten separate reovirus segments were attained, and these indicated the isolated agent was a MRV. Genetic and phylogenetic analyses based on the outer capsid sigma-1 (σ1) protein gene sequences supported the Florida white-tailed fawn isolate as a type 2 MRV that branched as the sister group to a MRV-2 strain previously characterized from the urine of a moribund lion (*Panthera leo*) in Japan. However, analyses based on 7/10 genes (L1-L2, M2-M3, S2-S4) supported the white-tailed deer MRV as the closest relative to a type 3 MRV strain isolated from a dead mink in China. These data suggest the white-tailed deer MRV may have resulted from the natural reassortment of MRVs originating from multiple wildlife species. To our knowledge, this is the first detection of MRV-2 infection in a white-tailed deer. Continued surveillance efforts are needed to determine whether this MRV-2 strain poses a health threat to farmed white-tailed deer populations.

1. Introduction

Deer farming is a fast growing industry in rural North America including Florida (Anderson et al., 2007). The industry generates more than $8 billion for the US economy and employs > 60,000 people (Anderson et al., 2017). As a relatively new livestock industry in North America, many of the pathogens that affect deer production are still unknown or understudied. Knowledge of potential diseases that may be encountered in deer farms is essential to ensure profitable deer production and to minimize the risk of spreading diseases to wildlife (Whitman, 2012). Recent investigations in Florida indicate that deer farming is largely hampered by hemorrhagic diseases, primarily caused by reovirus infections (Ahasan et al., 2018; Campbell and VerCauteren, 2011; Subramaniam et al., 2017).

The family *Reoviridae* includes viruses with segmented double-stranded RNA genomes enclosed within a multi-layered icosahedral

* Corresponding author at: Department of Infectious Diseases and Immunology, College of Veterinary Medicine, University of Florida, Gainesville, FL, USA.
E-mail address: tbwaltzek@ufl.edu (T.B. Waltzek).

https://doi.org/10.1016/j.virusres.2019.197642
Received 21 March 2019; Received in revised form 14 June 2019; Accepted 18 June 2019
Available online 19 June 2019
0168-1702/

capsid (Schiff et al., 2007). The non-enveloped virion varies from 65 to 80 nm in diameter, and contains 10 – 12 dsRNA segments. These segments are classified as large (L1, L2 and L3), medium (M1, M2, and M3) and small (S1, S2, S3, and S4) on the basis of the electrophoretic mobility (Knipe et al., 2013). Most of the virus genomic RNA (vRNA) segments are monocistronic though some segments have two or three in-frame initiation codons that lead to expression of additional open reading frames (ORFs) (Knipe et al., 2013). Reoviruses are known pathogens of deer, including those in Florida. Indeed, our group recently described isolation and complete virus genome sequence determinations of *Epizootic hemorrhagic disease virus*-1, -2, and -6 (EHDV-1, -2, and -6), which are reoviruses from the genus *Orbivirus* (Ahasan et al., 2018; Subramaniam et al., 2017). Moreover, serologic evidence of infection of Florida white-tailed deer (WD) (*Odocoileus virginianus*) with another orbivirus, Bluetongue virus (BTV), has previously been reported (Davidson et al., 1987).

Mammalian orthoreovirus (MRV) is a non-fusogenic prototype species of the genus *Orthoreovirus* that causes a range of respiratory, nervous, and enteric diseases of importance in human and veterinary medicine (Knipe et al., 2013). Mammalian orthoreoviruses are classified into four serotypes based on their genetic and antigenic relatedness: MRV type 1 Lang, type 2 Jones, type 3 Dearing, and type 4 Ndelle (Schiff et al., 2007). Haemagglutination and neutralization activities of MRVs are restricted to a single MRV gene segment, S1 gene that encodes the sigma-1 (σ1) protein, which is incorporated into the outer capsid layer of the virion (Weiner and Fields, 1977). The σ1 protein is responsible for viral attachment on cell receptors and determines the MRV serotype (Bassel-Duby et al., 1986). Studies have demonstrated that MRVs are prone to various types of genetic reassortment and intragenic rearrangement under laboratory and natural conditions (Dermody et al., 2013; Duncan, 1999; Wenske et al., 1985). The exchange of virus genomic RNA (vRNA) segments between MRV serotypes can lead to the evolution of new viruses with increased virulence and host range expansion (Chapell et al., 1994; Ouattara et al., 2011; Wenske et al., 1985). MRV serotypes are ubiquitously distributed and reported in a wide range of vertebrate hosts including mammals (Decaro et al., 2005; Hrdy et al., 1979; Knipe et al., 2013; Lelli et al., 2013; Lian et al., 2013), birds (Docherty et al., 1994; van den Brand et al., 2007) and reptiles (Ahne et al., 1987; Drury et al., 2002).

To date, orthoreovirus infections have not been reported in white-tailed deer or other cervids. Here, we report the isolation and characterization of a novel MRV-2 strain from a dead white-tailed deer fawn from central Florida.

2. Materials and methods

2.1. Animal history and specimens

In 2016, a farmed white-tailed deer fawn (animal OV204) from Webster County, Florida, began displaying clinical signs of illness one week post-parturition. Hours after birth the animal was given *Clostridium perfringens* C & D antitoxin (Colorado Serum Company) via intramuscular injection, a separate antitoxin with antibodies against *C. perfringens* Type C administered orally (Bovine Ecolizer + C20, Novartis/Elanco Products Co.), and colostrum with electrolytes administered orally (La Belle Colostrum Inc.). The fawn began having profuse foul-smelling diarrhea, and became lethargic and dehydrated several days prior to death at three-weeks-of age. During that time, it was treated with vitamin B-12 complex (Agri Laboratories, Ltd.), Ivomec (Ivermectin, Boehringer Ingelheim), Zactran (Gamithromycin, Merial Ltd.) and Excede (Ceftiofur, Zoetis Inc.). The fawn failed to improve and died within 48 h of treatment. A field necropsy was performed 24 h after the animal died and heart, liver, lung, kidney, and spleen tissues were collected. Sample collections and processing were conducted under approval of the Institutional Animal Care and Use Committee at University of Florida (IACUC Protocol #201609390).

2.2. Initial diagnostic evaluation

Kidney and lung tissues were submitted to the University of Florida College of Veterinary Medicine for bacteriological and mycological cultures. No tissues were evaluated by histopathology since necropsy was performed 24 h after death.

To determine whether one of the commonly encountered deer viruses might be the causative agent, RT-PCR was used to test whole blood and tissue homogenates for the vRNAs of EHDV, BTV, West Nile virus (WNV) and eastern equine encephalitis virus (EEEV).

Tissue homogenates (approx. 20 – 40 % w/v) were prepared by bead-beating heart, liver, and spleen tissues using a Biospec Mini-Beadbeater-16 (BioSpec Products, Inc., Bartlesville, OK). Briefly, 0.15 – 0.2 g of tissue was aseptically minced with scissors, then added to screw-capped 2 mL sterile polypropylene vials (BioSpec Products, Bartlesville, OK; Cat#: 10831) containing 0.75 gm high-density zirconium oxide 2 mm beads and 0.15 gm of high-density zirconium oxide 0.1 mm beads (both types of beads from Glen Mills, Clifton, NJ, Cat#: 7361-002000 and 7361-000100) (Crowder et al., 2010) and 500 µl of refrigerated Phosphate-Buffered Saline. After bead-beating for 2 min and 15 s, the vials were centrifuged at 8000 rpm (6000 x g) in a Thermo IEC MicroMax RF microcentrifuge for 5 min at 4 °C, and the resulting supernatant aseptically transferred to a sterile 1.5 mL cryovial, which was stored at −80 °C until further use.

Viral RNA was extracted from heart, liver, and spleen tissue homogenates using the QiaAmp Viral RNA mini kit (Qiagen, Valencia, California, USA), according to the manufacturer's protocol. For EHDV and BTV, an RT-qPCR multiplex assay based on a protocol described by Wernike et al. (2015) was used. In brief, the RT-qPCR was carried out using a VetMAX-Plus Multiplex One Step RT-PCR kit (Applied Biosystems, Foster City, California, USA), each individual multi-plex reaction in a total volume of 25 µL. For a single reaction, a mastermix containing 12.5 µL 2x RT-PCR buffer, 2.5 µL 10x multiplex RT-PCR enzyme mix, 0.375 µL RNAse-free water, 1 µL primer-probe mix, and 0.1 µL Xeno RNA [internal control] (Applied Biosystems) was prepared, into which was added 10 pmol of BTV forward and reverse primers, 2 pmol of BTV probe, 15 pmol of EHDV forward and reverse primers, and 2.5 pmol of EHDV probe.

For the detection of WNV and EEEV vRNAs, both assays were carried out using the VetMAX Plus One Step RT-PCR kit (Applied Biosystems, Foster City, California, USA), each in total reaction volumes of 25 µL. For a single reaction, a mastermix containing 12.5 µL 2x RT-PCR Buffer, 1 µL 25x RT-PCR enzyme, 1 µL nuclease free water, 1 µL Xeno Vic assay and 0.1 µL Xeno RNA [internal control] (Applied Biosystems) was prepared. For WNV, 25 pmol of forward and reverse primers and 5 pmol of probe (Lanciotti et al., 2000) were used. For EEEV, 18 pmol of forward and reverse primers and 5 pmol of probe (Lambert et al., 2003) were used. A total of 4 µL of template RNA was thereafter added to 21 µL of the mastermix containing either WNV or EEEV specific primers and probe.

The RT-qPCRs tests were performed in a 7500 fast Real-Time PCR System (Applied Biosystems, Foster City, California, USA) using the following thermal profiles: (a) For EHDV and BTV multiplex reactions: reverse transcription (RT) at 48 °C for 10 min, initial denaturation at 95 °C for 10 min, followed by 40 cycles of 3-step cycling consisting of denaturation at 95 °C for 15 s, annealing at 57 °C for 45 s, and extension at 68 °C for 45 s, (b) For WNV: RT at 48 °C for 10 min, initial denaturation at 95 °C for 10 min, followed by 40 cycles of 2-step cycling consisting of 95 °C for 15 s, and 60 °C for 45 s, and (c), For EEEV: RT at 48 °C for 10 min, initial denaturation at 95 °C for 10 min, followed by 40 cycles of 2-step cycling consisting of denaturation at 95 °C for 15 s, and at 60 °C for 45 s.

2.3. Cell culture

In addition to nucleic acid amplification, virus isolation from tissue

heart, liver, and spleen homogenates was attempted in Vero E6 cells (*Cercopithecus aethiops* [African green monkey], obtained from the American Type Culture Collection (ATCC, Manassas, VA, Cat#: ATCC CRL 1586) cells, which are susceptible and permissive for many strains of EHDV-1, -2, and -6, the agents presumed to be the major deer pathogens in central Florida. For this work, lung tissue was not available.

After thawing on ice, unfiltered 50 µl aliquots of the tissue homogenates were inoculated onto nearly confluent monolayers of Vero E6 in a 6-well Thermo Scientific Nunc cell-culture treated multidish (Thermo Fisher Scientific, Waltham, MA, cat#: 1483210) containing 50 µl of complete cell-growth medium consisting of Advanced Dulbecco's Modified Eagle's Medium (aDMEM) (Invitrogen Corp., Carlsbad, CA) supplemented with 10% heat-inactivated, gamma-irradiated, low-antibody fetal bovine serum (FBS) (GE Healthcare Life Sciences, Pittsburgh, PA, Cat#: SH30070.03IH), 2 mM L-Alanyl-L-Glutamine (GlutaMAX™, Invitrogen Corp.) and antibiotics (PSN; 50 µg/ml penicillin, 50 µg/ml streptomycin, 100 µg/ml neomycin [Invitrogen Corp.])]. Post-inoculation, the cells were incubated at 37 °C with 5% CO_2 with rocking every 15 min for 2 h. Thereafter, an additional 800 µl of complete cell-growth medium was added, the cells once again incubated at 37 °C with 5% CO_2. The inoculated cells were monitored daily for formation of virus-induced cytopathic effects (CPE), with re-feeds performed every three days with maintenance medium (aDMEM containing 3% FBS and regular amounts of other supplements). Mock-infected Vero E6 cells were maintained in parallel. In the laboratory, inoculated cells are routinely monitored daily for 30 days post-inoculation (dpi) before being judged negative for virus isolation.

2.4. Transmission electron microscopy (TEM)

Two nearly confluent T75 Corning cell-culture treated flasks (Thermo Fisher Scientific, Cat#: 07-202-000) of Vero E6 cells were each inoculated with 25 µl of first-passage cell lysate. The cells in one flask were fixed 3 dpi as described below for TEM to visualize the virus during early stages of CPE formation, the other 5 dpi for TEM using cells at a later stage of CPE development as: the infected cells were fixed in 15 mL of modified Karnovsky's fixative (2P + 2 G, 2% formaldehyde prepared from paraformaldehyde and 2% glutaraldehyde in 0.1 M cacodylate buffer pH 7.4) at room temperature for 2 h. After fixation, the cells were scraped from the flask and transferred into a 15 mL conical tube and centrifuged at 3000 × g for 10 min at 4 °C. The fixative was discarded and the pelleted cells re-suspended in 1 mL cacodylate buffer and stored at 4 °C for three days before being shipped to University of Texas Medical Branch Electron Microscopy Laboratory at (UTMB-EML).

At UTMB-EML, the cell pellets were washed in cacodylate buffer and left in 2P + 2 G fixative overnight at 4 °C. The next day they were washed twice in cacodylate buffer, post-fixed in 1% OsO_4 in 0.1 M cacodylate buffer pH 7.4, *en bloc* stained with 2% aqueous uranyl acetate, dehydrated in ascending concentrations of ethanol, processed through propylene oxide and embedded in Poly/Bed 812 epoxy plastic (Polysciences, Warrington, PA). Ultrathin sections (~75 nm) were cut on Leica ULTRACUT EM UC7 ultra-microtome (Leica Microsystems, Buffalo Grove, IL), stained with 0.4% lead citrate and examined in JEM-1400 electron microscope (JEOL USA, Peabody, MA) at 80 kV.

2.5. Determination of complete coding sequences of Mammalian orthoreovirus type 2 strain OV204 (MRV2-WD-OV204)

The complete coding regions of the MRV2-WD-OV204 was sequenced using a next-generation Illumina MiSeq sequencer. Briefly, 1 mL of passage 1 cell lysate was thawed on ice and centrifuged at 5509 × g for 20 min at 4 °C in a Beckman J2-MI centrifuge to remove cell debris. Virus particles were then pelleted from the clarified supernatant by ultracentrifugation at 100,000 × g for 90 min at 4 °C using a Beckman JA-14 fixed angle rotor. The supernatant was pipetted off and the pelleted virus resuspended in resuspension buffer (10 mM Tris-HCl, pH 7.6, 10 mM KCl, 1.5 mM $MgCl_2$) and treated with Baseline-ZERO DNase (Lucigen, Middleton, WI, USA), an exonuclease used to digest extraneous ds- and ssDNA to mononucleotides. The virus genomic RNA (vRNA) was subsequently purified using a QIAamp viral RNA mini kit (Qiagen). The vRNA served as a template to construct a cDNA library using an NEBNext Ultra RNA Library Prep Kit (New England BioLabs® Inc.) followed by sequencing on an Illumina MiSeq sequencer using a version 3 chemistry 600 cycle kit.

2.6. Genome assembly and annotation

Paired-end reads obtained from Illumina MiSeq were quality trimmed in CLC Genomic Workbench 10.1.1 and assembled *de novo* using SPAdes 3.5.0 genome assembly algorithm (Bankevich et al., 2012) with default parameters. The assembled contigs were then screened against a proprietary viral database using BLASTX in CLC Genomic Workbench 10.1.1. BLASTX searches revealed the highest identities of assembled contigs to mammalian orthoreoviruses (MRVs). Putative open reading frames (ORFs) for the novel white-tailed deer MRV genome were predicted using GeneMarkS (http://exon.biology.gatech.edu/) (Besemer et al., 2001) restricting the search to viral sequences. Additionally, the functions of the genes were predicted using BLASTP searches against the NCBI non-redundant protein database.

2.7. Genetic and phylogenetic analyses

A Maximum Likelihood (ML) analysis was generated using the nucleotide (nt) sequence of the outer capsid protein (σ1) gene of the novel MRV2-WD-OV204 compared to 26 orthoreoviruses whose sequences were deposited in GenBank (including MRV2-WD-OV204). However, ML analyses using the other nine segments (L1-L3, M1-M3 and S2-S4) of the novel MRV2-WD-OV204 were compared to 24 orthoreoviruses for which complete coding sequences were available in GenBank. The nt sequences were aligned using MAFFT (Katoh et al., 2005) and the ML analyses was performed in IQ-TREE V 1.14.1 with default settings and 1000 non-parametric bootstraps to test the robustness of the hypothesis (Nguyen et al., 2015). A sequence identity matrix was constructed based on the nucleotide alignment of the outer capsid protein (σ1) gene for the same 26 orthoreoviruses in the Sequence Demarcation Tool v.1.2 (Muhire et al., 2014) using the MAFFT alignment option.

3. Results

3.1. Bacteriology and mycology

Upon aerobic culture, alpha-hemolytic streptococci > 99%, *Escherichia coli* < 1%, enteric Gram negative bacilli and non-hemolytic staphylococci in the kidney, and alpha-hemolytic streptococci > 99%, *Escherichia coli* < 1% and Gram positive coccobacilli in the lungs were isolated. Additionally, mixed bacterial flora, including *Fusobacterium varium* in the kidney, and mixed bacterial flora, including *Peptoniphilus* sp. in the lung, were isolated in anaerobic cultures. These bacteriology findings were considered insignificant and judged to be overgrowth by contaminating bacteria acquired during field necropsy.

No fungal agent was identified in the lung and kidney specimens processed for mycological examination.

3.2. Cell culture and electron microscopy

Evidence of virus-induced CPE were first observed 7 dpi of Vero E6 cells with the spleen homogenates (only). The CPE were pronounced 10 dpi, and extensive the following day, when the cells were scraped. Cytopathic effects initially consisted of formation of cytoplasmic inclusions and granulation of the cells followed by detachment of dead cell from the growing surface (Fig. 1). Both scraped cells and cell lysate were collected and frozen at −80 °C until further use.

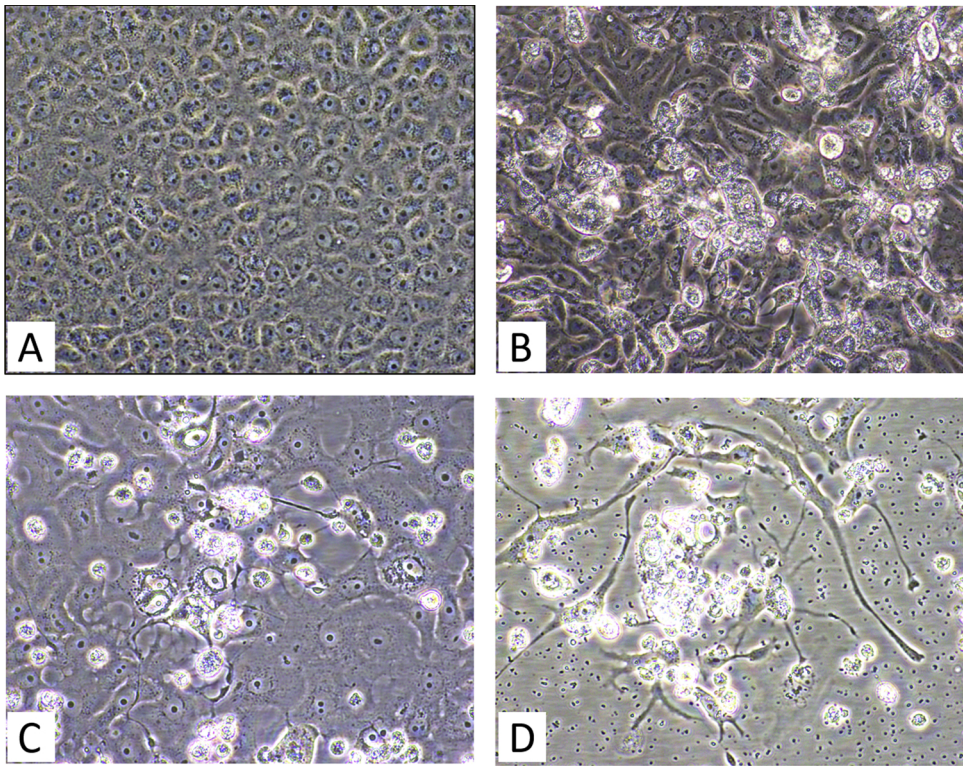

Fig. 1. Vero E6 cells inoculated with spleen homogenate from OV204. (A) Mock-infected cells, 11 days post-seed. (B) Appearance of cells inoculated with spleen homogenate 6 days post inoculation (dpi). Infected cells in the process of apoptosis were evident, appearing refractile. (C) By 10 dpi, perinuclear darkening of the cytoplasm, cytoplasmic inclusions, and elongation and "spindling" of some cells, were observable prior to apoptosis of infected cells. Gaps in the monolayer resulting from the detachment of dead cells was also evident. (D) At 11 dpi, much of the monolayer had been killed. Most of the remaining attached cells were elongated, and debris resulting from apoptosis was abundant. Original images taken at 400X magnification.

Ultrastructural examination of virus particles in an ultrathin section of infected Vero E6 cells done by TEM revealed the presence of icosahedral non-enveloped virus particles within the cytoplasm of Vero cells 3 dpi (Fig. 2A). Moreover, a fragment of an infected Vero E6 cell revealed with a virus factory contained particles in different stages of maturation and empty capsid shells (Fig. 2B). The intracytoplasmic virus particles were approximately ~75 nm in diameter, and occasionally arranged in paracrystalline arrays within infected cell cytoplasm (Fig. 2C-E). The lysing infected Vero E6 cells phagocytized by neighboring cells were often observed (Fig. 2F and fig. S1).

3.3. Complete genome sequencing, assembly and genome annotation

The MiSeq data resulted in a total of 3,073,750 pair-end reads and a total of 3,072,702 high quality reads were identified after quality trimming in CLC Genomic Workbench 10.1.1 using default parameters. *De novo* assembly of the paired-end reads followed by BLASTX analyses recovered all 10 segments of the novel white-tailed deer MRV. The average coverage of the MRV genome was 670 reads/nucleotide (nt) and the coverage for each segment ranged between 195 and 2,111 reads/nt. These segments were accessioned to the GenBank database (accession numbers MK092964-MK092973). The sizes of the 10 different segments, and the inferred length of structural and non-structural proteins are summarized in Table 1.

3.4. Genetic and phylogenetic analyses

Based on the nucleotide alignments of seven genes (L1-L2, M2-M3, S2-S4), MRV2-WD-OV204 demonstrated highest nucleotide identities (98–99%) to a MRV3 strain isolated from a farmed mink in China (Table 2). The MRV2-WD-OV204 S1, M1, and L3 gene alignments displayed highest identities to a MRV2 strain isolated from a moribund lion in Japan (93%), a MRV2 strain isolated from a common vole (*Microtus arvalis*) in Hungary (91%), and a MRV3 strain isolated from bat (*Hipposideros* sp.) in China (99%), respectively (Fig. 3 and Table 2). Similar to the genetic analyses, the phylogenetic analyses based on the same seven genes supported WD-OV204 as the closest relative to a MRV-3 strain isolated from a farmed mink (Fig. 4, S2-S3, S6-S7 and S8-S10). This relationship was poorly supported in the S4 gene tree (Fig. S10). Similar to the genetic analyses, the MRV2-WD-OV204 S1and L3 gene trees supported WD-OV204 as the closest relative to a MRV-2 strain isolated from a lion in Japan and MRV-3 strains isolated from Rickett's big-footed bat (*Myotis ricketti*) in China, respectively (Fig. 4 and S4). Although poorly supported, the M1 gene tree displayed MRV2-WD-OV204 as the sister group to a clade formed from MRV-2 strains isolated from a common vole in Hungary and a human in the United States (Fig. S5).

4. Discussion

To our knowledge, this study provides the first characterization of a MRV in a cervid host, a moribund white-tailed deer on a Florida farm. The sequence data generated in this study will assist in the development of molecular diagnostic tools for future epidemiological investigations into the prevalence of MRV2-WD-OV204 in Florida white-tailed deer populations. Future cases of MRV2-WD-OV204 in white-tailed deer would benefit from the development of diagnostics to assist in determining its pathogenicity by quantifying microscopic lesions (e.g., histopathological examination complemented by an *in situ* hybridization assay), viral load (e.g., TaqMan quantitative PCR assay), and viral titer (e.g., 50% tissue culture infectious dose assay or plaque forming unit assay).

Like other MRVs, MRV2-WD-OV204 is non-fusogenic in cell culture (Fig. 1) and displays the virion morphology and morphogenesis of a reovirus (Fig. 2). Genetic and phylogenetic analyses based on 7/10 genes (L1-L2, M2-M3, S2-S4) supported MRV2-WD-OV204 as the closest relative to MRV3-SD-14 isolated from a dead mink in China in 2014 (Zhang et al., 2016). In contrast, genetic and phylogenetic analyses based on the S1 gene supported MRV2-WD-OV204 as a member of the MRV2 serotype most closely related to an unpublished MRV2 isolated from the urine of a lion in 2011 (GenBank accession no. LC121909.1). These data suggest MRV2-WD-OV204 may have resulted from the

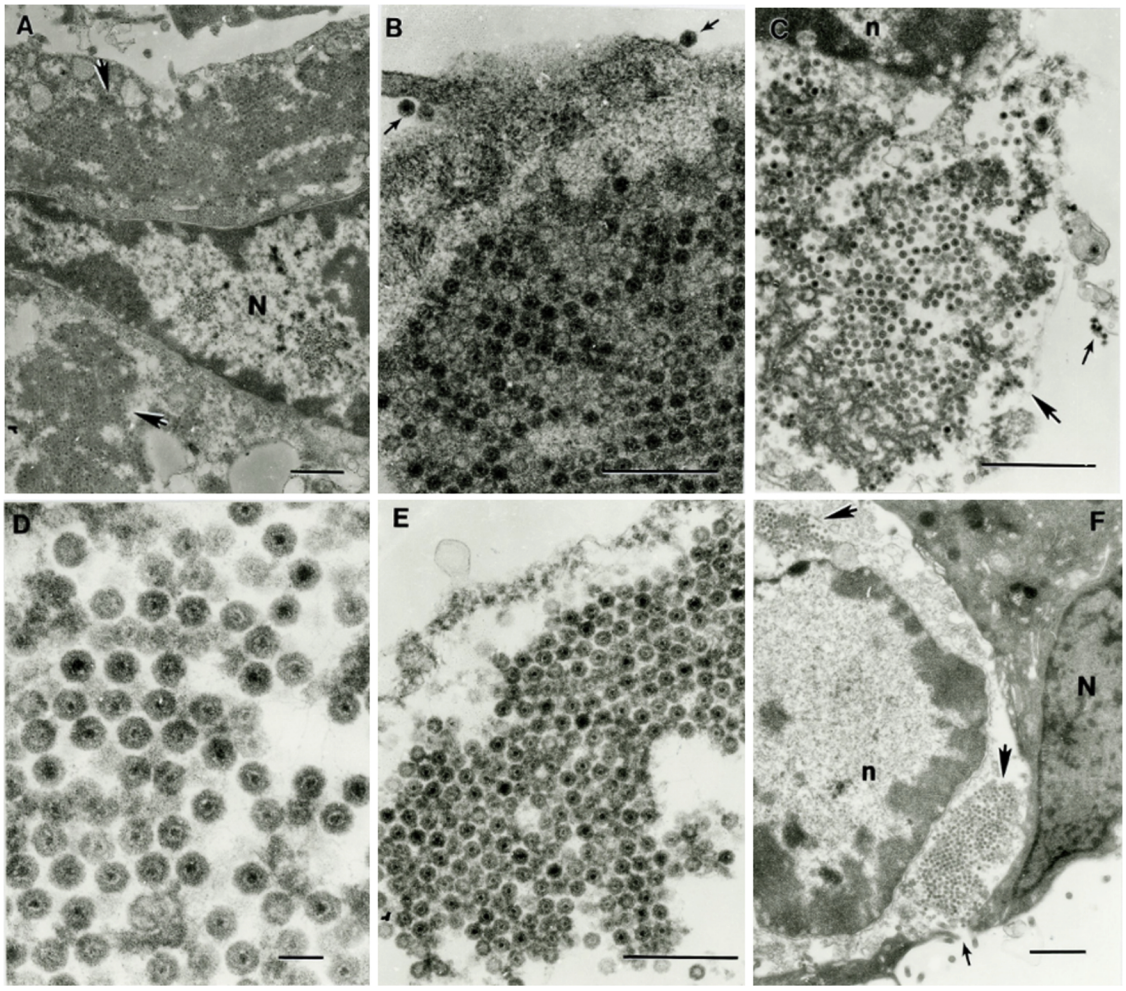

Fig. 2. Ultrastructure of MRV2-WD-OV204 in ultrathin sections of infected Vero E6 cells. (A) Cell with two prominent cytoplasmic viral inclusions (virus factories) (arrows). N; host cell nucleus. Bar = 1 µm. (B) Fragment of an infected cell with a virus factory containing particles in different stages of maturation and empty capsid shells. Arrows indicate attached virions at the cell surface. Bar = 0.5 µm. (C) Lysed Vero cells 3 dpi with a nucleus (n) with chromatin condensed at its periphery, disorganized cytoplasm and plasma membrane releasing virions into the medium (arrow). Small arrow indicates extracellular virions attached to a cell fragment. Bar = 1 µm. (D) Virions within the inclusion 3 dpi. Bar = 100 nm. (E) Fragment of an infected cell with virus particles arranged in a paracrystalline array. Bar = 0.5 µm. (F) Fragment of a Vero cell (N indicates part of its nucleus) phagocytizing a lysed infected cell (n – indicates its nucleus) with two viral inclusions (big arrows) and virus particles being released into the medium (small arrow). Bar = 1 µm.

Table 1
Sizes of the 10 segments and inferred length of structural, and non-structural proteins of the novel MRV2-WD-OV204 isolate.

Segments	Segment Size (nt)	ORF/Protein		
		Class	Size (aa)	Protein functions
L1	3804 bp	λ3	1267	RNA-dependent RNA polymerase
L2	3870 bp	λ2	1289	Guanyltransferase, methyltransferase
L3	3748 bp	λ1	1275	RNA binding, NTPase, heliease, RNA triphosphatase
M1	2211 bp	µ2	736	Binds RNA NTPase
M2	2127 bp	µ1	708	Cell penetration, transcriptase activation
M3	2154 bp	µNS	726	Unknown NS
S1	1387 bp	σ1	461	Cell attachment
S2	1257 bp	σ2	418	Bind dsRNA
S3	1101 bp	σNS	366	Inclusion formation, binds ssRNA
S4	1098 bp	σ3	365	Binds dsRNA

Note: nt, nucleotide; aa, amino acid.

natural reassortment of a farmed mink MRV3 and one or more MRVs originating from wildlife species (e.g., lion, common vole, bat). A case of genetic reassortment between strains of MRV2 and MRV3 in bats from China has been reported previously (Wang et al., 2015). Accumulating evidence suggests intragenic rearrangement and reassortment is commonplace among MRVs infecting pigs, bats, mink, and humans (Wang et al., 2015; Yang et al., 2015). Viral reassortment is a mechanism that may lead to newly emerging pandemic reoviruses with negative consequences on human and animal populations (McDonald et al., 2016).

The close genetic relationship of MRVs from deer in Florida and mink in China may suggest international trade has played a role in the dissemination of these reoviruses. American mink (*Neovision vision*) may have carried MRV to China during the development of the Chinese fur industry that began in 1956 (Sha et al., 2011). Genetically uncharacterized reoviruses have been isolated from farmed American mink in China since 1992 (Liu et al., 1992). However, American mink have been farmed for their fur in North America since the late 1880s and MRV has yet to be reported in managed or wild populations. Furthermore, it is difficult to understand how the deer reported in our study became infected with MRV unless it was exposed to an MRV-infected American mink on the farm. Ultimately, the source of infection

Table 2
Nucleotide/amino acid identities for each gene segment of the novel MRV2-WD-OV204 compared to selected orthoreoviruses.

WD-OV204	Human MRV prototype strains, %				Swine reovirus strains, %		Wildlife reovirus strains, %				
	T1L	T2J	T3D	T4N	GD-1	SC-A	Bat (WIV2)	Common vole (MORV/47Ma/06)	Lion	Mink (SD-14)	Mink (HB-A)
L1	89.0/98.1	75.6/92.4	89.2/98.5	89.8/97.8	96.0/98.8	96.3/99.2	90.2/99.3	88.4/98.5	96.3/99.3	**98.6/99.9**	96.4/99.3
L2	86.3/96.9	72.8/87.1	77.5/93.4	NA	97.5/98.7	96.5/98.3	95.8/98.8	85.4/97.0	95.6/98.9	**98.8/99.5**	95.2/99.0
L3	84.3/98.8	77.4/95.8	84.3/98.5	NA	95.3/99.2	95.9/99.1	**99.2/99.8**	87.5/98.8	96.1/99.7	98.3/99.8	97.6/99.4
M1	88.3/96.7	71.6/81.3	88.2/96.1	NA	86.8/95.1	88.1/95.4	87.7/96.2	**91.0/97.2**	88.2/95.8	88.7/95.8	87.6/95.0
M2	84.8/98.2	76.3/97.2	89.7/97.7	88.9/98.3	**98.8/99.3**	95.3/99.0	89.1/98.7	89.8/98.9	95.9/99.4	**98.8/99.6**	96.2/99.3
M3	84.8/95.2	70.7/82.3	85.1/95.2	NA	83.8/94.2	96.0/97.5	96.6/97.9	84.4/95.2	96.2/98.2	**97.6/98.0**	96.4/97.9
S1	68.4/53.4	63.5/57.1	HD/28.6	HD/28.9	HD/27.9	HD/27.9	HD/53.2	68.2/70.7	**92.5/95.7**	HD/25.1	67.9/53.8
S2	95.9/99.5	77.2/94.3	84.9/99.3	85.5/97.9	84.3/98.3	85.9/99.3	**99.1/99.5**	85.8/98.3	85.8/99.3	**99.5/100**	98.9/99.3
S3	90.2/97.3	74.6/85.8	85.0/96.7	NA	88.5/97.3	89.0/97.0	95.7/98.4	86.1/97.0	95.9/98.1	**98.9/99.2**	95.6.097.5
S4	87.0/96.7	79.3/92.1	86.6/96.7	90.7/96.4	76.3/86.3	98.0/99.2	96.8/98.6	85.6/96.7	97.3/99.2	**98.8/99.5**	97.2/99.2

T1L, type 1 Lang (accession nos.: M24734, AF378003, AF129820, AF461682, AF490617, AF174382, EF494445, L19774, M14325, M13139); T2J, type 2 Jones (accession nos.: M31057, AF378005, AF129821, AF124519, M19355, AF174383, M10261, L19775, M18390, X60066); T3D, type 3 Dearing (accession nos.: HM159613-22); T4N, type 4 Ndelle (accession nos.: AF368033-37); GD-1, MRV type 3 (accession nos.: JX486057-66); SC-A, MRV (accession nos.: DQ997719, DQ885990, EF029088, DQ396804, DQ482462, DQ403254, DQ911244, DQ396805, DQ411553, DQ396806); Bat (WIV2), MRV type 1 isolate WIV2 (accession nos.: KT444522-31); Common vole (MORV/47Ma/06), MRV type 2 strain MORV/47Ma/06 (accession nos.: KX384846-55); Lion, MRV type 2 isolate (accession nos.: LC121909-18); Mink (SD-14), MRV type 3 strain SD-14 (accession nos.: KT224504-13); Mink (HB-A), MRV type 3 strain HB-A (accession nos.: KC462149-58); L, Large segment; M, medium segment; S, small segment; NA, not available; HD, highly dissimilar as query cover < 2%. Boldface indicates highest sequence identity.

on the deer farm will likely remain a mystery and may have involved exposure to a yet unknown infected mammalian host (e.g., rodent, felid, human, bat). This study underscores the need for continued surveillance and genomic characterization of MRVs from farmed and wildlife species as a way of better understanding their evolution, epidemiology, and zoonotic potential.

Mammalian orthoreoviruses are known causative agents of gastrointestinal, respiratory, and neurological infections in both humans and animals (Dermody et al., 2013). Studies have been demonstrated an age-dependent increase in reovirus-specific antibodies in children 1 year of age and older. (Tai et al., 2005). MRV3 has been reported to be associated with meningitis in a child (Ouattara et al., 2011; Tyler et al., 2004). Mortality due to MRV infections was highest in mink < 3 months of age (Lian et al., 2013). Interestingly, the white-tailed deer fawn infected with MRV2 died when it was only three weeks old. Orthoreoviruses, similar to other reoviruses (e.g., rotaviruses), appear to

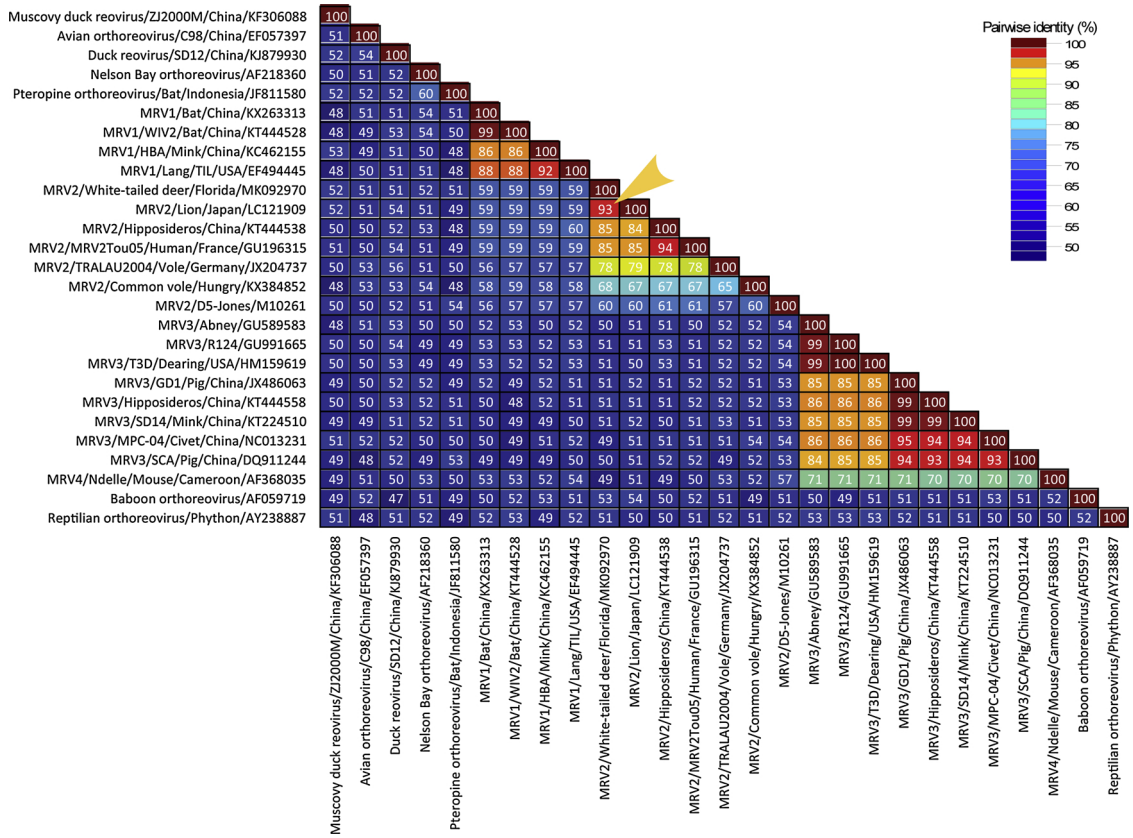

Fig. 3. Sequence identity matrix showing the nucleotide percent similarity of the novel MRV2-WD-OV204 to 26 other orthoreoviruses based on the S1 gene. The identities ranged from 46 to 93% and the highest identity (yellow arrow) was observed with a MRV-2 strain previously characterized from the urine of a moribund lion in Japan.

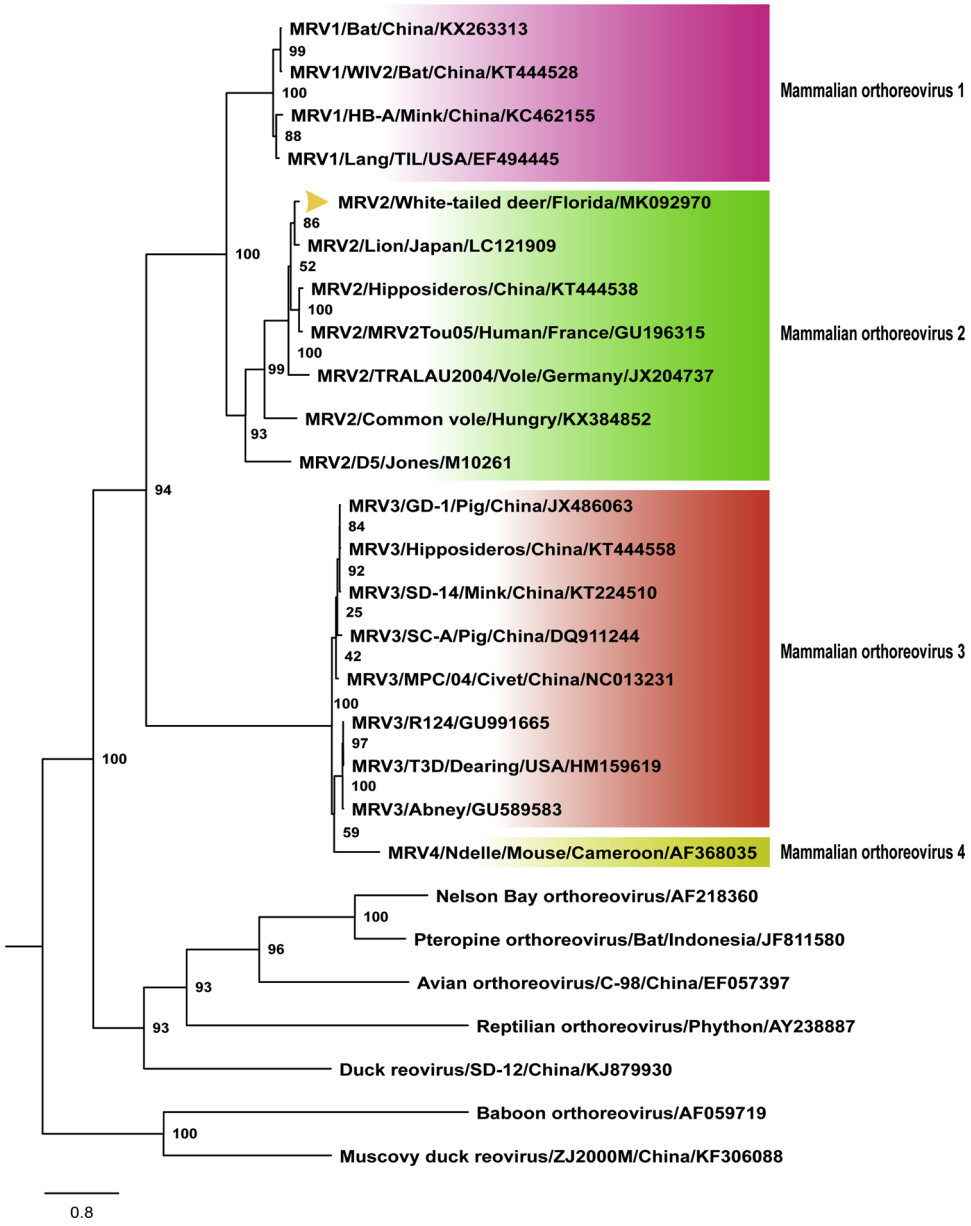

Fig. 4. Maximum Likelihood phylogram depicting the relationship of the novel MRV2-WD-OV204 to representatives of the *Orthoreovirus* genus based on the aligned nucleotide sequences of the S1 gene. Bootstrap values are given at each node and the branch lengths represent the number of inferred substitutions as indicated by the scale.

cause disease in children and young animals.

The farmed deer in this study and a Chinese farmed mink infected with a related MRV serotype displayed evidence of gastrointestinal disease (e.g., emaciation and diarrhea) prior to death (Zhang et al., 2016). However, neither study performed pathological examinations to determine the role of the respective MRV serotypes in the gastrointestinal diseases. Future challenge experiments are needed to determine whether MRV2-WD-OV204 can establish a lethal gastrointestinal disease in white-tailed deer, as well as other wildlife and domesticated species.

Ethical approval

All animal procedures were reviewed and approved by the Institutional Animal Care and Use Committee at University of Florida (IACUC Protocol # 201609390).

Declaration of Competing Interest

All the authors declare that they have no conflict of interest.

Funding

This study was funded by the University of Florida, Institute of Food and Agricultural Sciences Cervidae Health Research Initiative, with funds provided by the State of Florida legislature.

Appendix A. Supplementary data

Supplementary material related to this article can be found, in the online version, at doi:https://doi.org/10.1016/j.virusres.2019.197642.

References

Ahasan, M.S., Subramaniam, K., Lednicky, J.A., Loeb, J.C., Sayler, K.A., Wisely, S.M., Waltzek, T.B., 2018. Complete genome sequence of epizootic hemorrhagic disease virus serotype 6, isolated from Florida white-Tailed deer (*Odocoileus virginianus*). Genome Announc. 6 (14) e00160-00118.

Ahne, W., Thomsen, I., Winton, J., 1987. Isolation of a reovirus from the snake, Python regius. Arch. Virol. 94 (1-2), 135–139.

Anderson, D.P., Frosch, B.J., Outlaw, J.L., 2007. Economic Impact of the United States Cervid Farming Industry. Agricultural and Food Policy Center, Texas A&M University, College Station, TX.

Anderson, D.P., Outlaw, J.L., Earle, M., JW, R., 2017. Agricultural and Food Policy Center, Texas A&M University System, Research Reoprt 17-4. Economic impact of U.S. deer breeding and hunting operations.

Bankevich, A., Nurk, S., Antipov, D., Gurevich, A.A., Dvorkin, M., Kulikov, A.S., Lesin, V.M., Nikolenko, S.I., Pham, S., Prjibelski, A.D., Pyshkin, A.V., Sirotkin, A.V., Vyahhi, N., Tesler, G., Alekseyev, M.A., Pevzner, P.A., 2012. SPAdes: a new genome assembly algorithm and its applications to single-cell sequencing. J. Comput. Biol. 19 (5), 455–477.

Bassel-Duby, R., Spriggs, D., Tyler, K., Fields, B., 1986. Identification of attenuating mutations on the reovirus type 3 S1 double-stranded RNA segment with a rapid sequencing technique. J. Virol. 60 (1), 64–67.

Besemer, J., Lomsadze, A., Borodovsky, M., 2001. GeneMarkS: a self-training method for prediction of gene starts in microbial genomes. Implications for finding sequence motifs in regulatory regions. Nucleic Acids Res. 29 (12), 2607–2618.

Campbell, T.A., VerCauteren, K., 2011. Diseases and parasites of White-tailed deer. In: David, G. (Ed.), Biology and Management of White-Tailed Deer. CRC Press, Boca Raton, pp. 219–249.

Chapell, J., Goral, M.I., Rodgers, S.E., Dermody, T., 1994. Sequence diversity within the reovirus S2 gene: reovirus genes reassort in nature, and their termini are predicted to form a panhandle motif. J. Virol. 68 (2), 750–756.

Crowder, C.D., Rounds, M.A., Phillipson, C.A., Picuri, J.M., Matthews, H.E., Halverson, J., Schutzer, S.E., Ecker, D.J., Eshoo, M.W., 2010. Extraction of total nucleic acids from ticks for the detection of bacterial and viral pathogens. J. Med. Entomol. 47 (1), 89–94.

Davidson, W.R., Blue, J.L., Flynn, L.B., Shea, S.M., Marchinton, R.L., Lewis, J.A., 1987. Parasites, diseases and health status of sympatric populations of sambar deer and white-tailed deer in Florida. J. Wildl. Dis. 23 (2), 267–272.

Decaro, N., Campolo, M., Desario, C., Ricci, D., Camero, M., Lorusso, E., Elia, G., Lavazza, A., Martella, V., Buonavoglia, C., 2005. Virological and molecular characterization of a mammalian orthoreovirus type 3 strain isolated from a dog in Italy. Vet. Microbiol. 109 (1-2), 19–27.

Dermody, T., Parker, J., Sherry, B., 2013. Orthoreoviruses. In: In: Knipe, D.M., Howley, P.M., Griffin, D., Lamb, R., Martin, M., Roizman, B., Straus, S. (Eds.), Fields Virology. Vol. 2 Lippincott Williams & Wilkins.

Docherty, D., Converse, K., Hansen, W., Norman, G., 1994. American woodcock (Scolopax minor) mortality associated with a reovirus. Avian Dis. 899–904.

Drury, S., Gough, R., Welchman, Dd.B., 2002. Isolation and identification of a reovirus from a lizard, Uromastyx hardwickii, in the United Kingdom. British Medical Journal Publishing Group.

Duncan, R., 1999. Extensive sequence divergence and phylogenetic relationships between the fusogenic and nonfusogenic orthoreoviruses: a species proposal. Virology 260 (2), 316–328.

Hrdy, D., Rosen, L., Fields, B., 1979. Polymorphism of the migration of double-stranded RNA genome segments of reovirus isolates from humans, cattle, and mice. J. Virol. 31 (1), 104–111.

Katoh, K., Kuma, K., Toh, H., Miyata, T., 2005. MAFFT version 5: improvement in accuracy of multiple sequence alignment. Nucleic Acids Res. 33 (2), 511–518.

Knipe, D.M., Howley, P.M., Griffin, D., Lamb, R., Martin, M., Roizman, B., Straus, S., 2013. Fields Virology (Sixth Edition), sixth edition. ed. Philadelphia (EUA): Lippincott Williams & Wilkins, 2. Lippincott Williams & Wilkins, Philadelphia.

Lambert, A.J., Martin, D.A., Lanciotti, R.S., 2003. Detection of North American eastern and western equine encephalitis viruses by nucleic acid amplification assays. J. Clin. Microbiol. 41 (1), 379–385.

Lanciotti, R.S., Kerst, A.J., Nasci, R.S., Godsey, M.S., Mitchell, C.J., Savage, H.M., Komar, N., Panella, N.A., Allen, B.C., Volpe, K.E., 2000. Rapid detection of West Nile virus from human clinical specimens, field-collected mosquitoes, and avian samples by a TaqMan reverse transcriptase-PCR assay. J. Clin. Microbiol. 38 (11), 4066–4071.

Lelli, D., Moreno, A., Lavazza, A., Bresaola, M., Canelli, E., Boniotti, M., Cordioli, P., 2013. Identification of Mammalian orthoreovirus type 3 in Italian bats. Zoonoses Public Hlth 60 (1), 84–92.

Lian, H., Liu, Y., Zhang, S., Zhang, F., Hu, R., 2013. Novel orthoreovirus from mink, China, 2011. Emerg. Infect Dis. 19 (12), 1985.

Liu, W., Han, H., Yang, S., Yao, Q., Zhou, X., Zhang, Z., 1992. Isolation, identification and pathogenicity of the enteric reovirus from mink [in Chinese]. Fur-Anim. Breed. 14, 1–3.

McDonald, S.M., Nelson, M.I., Turner, P.E., Patton, J.T., 2016. Reassortment in segmented RNA viruses: mechanisms and outcomes. Nat. Rev. Microbiol. 14 (7), 448.

Muhire, B.M., Varsani, A., Martin, D.P., 2014. SDT: a virus classification tool based on pairwise sequence alignment and identity calculation. PLoS One 9 (9), e108277.

Nguyen, L.T., Schmidt, H.A., von Haeseler, A., Minh, B.Q., 2015. IQ-TREE: a fast and effective stochastic algorithm for estimating maximum-likelihood phylogenies. Mol. Biol. Evol. 32 (1), 268–274.

Ouattara, L.A., Barin, F., Barthez, M.A., Bonnaud, B., Roingeard, P., Goudeau, A., Castelnau, P., Vernet, G., Paranhos-Baccalà, G., Komurian-Pradel, F., 2011. Novel human reovirus isolated from children with acute necrotizing encephalopathy. Emerg. Infect Dis. 17 (8), 1436.

Schiff, L., Nibert, M.L., Tyler, K.L., 2007. Orthoreoviruses and their replication. Fields Virol. 5, 1853–1915.

Sha, L., Xu, Y.-P., Jin, L.-J., 2011. A review of mink farming practices in China. Scientifur 35 (3), 27–37.

Subramaniam, K., Lednicky, J.A., Loeb, J., Sayler, K.A., Wisely, S.M., Waltzek, T.B., 2017. Genomic sequences of epizootic hemorrhagic disease viruses isolated from Florida White-tailed deer. Genome Announc. 5 (43) e01174-01117.

Tai, J.H., Williams, J.V., Edwards, K.M., Wright, P.F., Crowe Jr, J.E., Dermody, T.S., 2005. Prevalence of reovirus-specific antibodies in young children in Nashville, Tennessee. J. Infect. Dis. 191 (8), 1221–1224.

Tyler, K.L., Barton, E.S., Ibach, M.L., Robinson, C., Campbell, J.A., O'donnell, S.M., Valyi-Nagy, T., Clarke, P., Wetzel, J.D., Dermody, T.S., 2004. Isolation and molecular characterization of a novel type 3 reovirus from a child with meningitis. J. Infect. Dis. 189 (9), 1664–1675.

van den Brand, J.M., Manvell, R., Paul, G., Kik, M.J., Dorrestein, G.M., 2007. Reovirus infections associated with high mortality in psittaciformes in the Netherlands. Avian Pathol. 36 (4), 293–299.

Wang, L., Fu, S., Cao, L., Lei, W., Cao, Y., Song, J., Tang, Q., Zhang, H., Feng, Y., Yang, W., 2015. Isolation and identification of a natural reassortant mammalian orthoreovirus from least horseshoe bat in China. PLoS One 10 (3), e0118598.

Weiner, H.L., Fields, B., 1977. Neutralization of reovirus: the gene responsible for the neutralization antigen. J. Exp. Med. 146 (5), 1305–1310.

Wenske, E.A., Chanock, S., Krata, L., Fields, B., 1985. Genetic reassortment of mammalian reoviruses in mice. J. Virol. 56 (2), 613–616.

Wernike, K., Hoffmann, B., Beer, M., 2015. Simultaneous detection of five notifiable viral diseases of cattle by single-tube multiplex real-time RT-PCR. J. Virol. Methods 217, 28–35.

Whitman, B.J., 2012. White-tailed deer movement and habitat interactions prior to death in Central New York. State University of New York College of Environmental Science and Forestry.

Yang, X.-L., Tan, B., Wang, B., Li, W., Wang, N., Luo, C.-M., Wang, M.-N., Zhang, W., Li, B., Peng, C., 2015. Isolation and identification of bat viruses closely related to human, porcine and mink orthoreoviruses. J. Gen. Virol. 96 (12), 3525–3531.

Zhang, Y.-w., Liu, Y., Lian, H., Zhang, F., Zhang, S.-f., Hu, R.-l., 2016. A natural reassortant and mutant serotype 3 reovirus from mink in China. Arch. Virol. 161 (2), 495–498.